*Solid State Science and Technology, Vol. 24, No 1 (2016) 220-230*
ISSN 0128-7389 | *http://journal.masshp.net*

# STRUCTURAL, ELECTRONICS AND OPTICAL PROPERTIES STUDY OF Gd-DOPED $TiO_2$ FOR DYE SENSITIZED SOLAR CELL

N.S. Azhar[1,2], M.H. Samat[1,2], N. Hamzah[3], M.F.M. Taib[1,2], R. Zakaria[1], O.H. Hassan[2,4], M.Z.A. Yahya[2,5] and A.M.M. Ali[1,2]

[1]*Faculty of Applied Sciences, Universiti Teknologi MARA, 40450 Shah Alam, Selangor, Malaysia*

[2]*Ionics Materials & Devices Research Laboratory (iMADE), Institute of Science, Universiti Teknologi MARA, 40450 Shah Alam, Selangor, Malaysia*

[3]*Center of Foundation Studies, Universiti Teknologi MARA, 42300 Puncak Alam, Selangor, Malaysia*

[4]*Department of Industrial Ceramics, Faculty of Art & Design, Universiti Teknologi MARA, 40450 Shah Alam, Selangor, Malaysia*

[5]*Faculty of Defence Science & Technology, Universiti Pertahanan Nasional Malaysia, 57000 Kuala Lumpur, Malaysia*

*Corresponding author: ammali@salam.uitm.edu.my*

## ABSTRACT

In this article, the pure anatase titanium dioxide ($TiO_2$) and anatase $TiO_2$ doped with gadolinium (Gd) were computed using first principles with the plane-wave ultrasoft pseudopotentials method based on the density functional theory (DFT). The calculated results demonstrate that the mixing of Gd dopants induces states with pure Ti 3*d* and $O_2$ 2*p* valence band attributes to the band gap narrowing from 2.153 eV to 0.247 eV which could play an important role in enhancing the catalytic activity and visible light absorbtion of anatase $TiO_2$. The optical absorption shifted from UV region to visible light region. The properties from first-principles study shown in Gd-doped $TiO_2$ can enhance the efficiency of DSSC because more visible light can be absorb from the doping effect in $TiO_2$. The above results would be quite helpful for research guiding and further developing of $TiO_2$ photocatalyst.

*Keywords: Electronic; Optical; DSSC; First-Principles;*

## INTRODUCTION

Dye-sensitized solar cell (DSSC) is one of the photoelectrochemical solar devices which made of a thin film solar cell with high performance that expected to be economically viable energy devices. The DSSC made up by five components namely

mechanical support coated with transparent conductive oxide, a semiconductor film, a sensitizer that adsorbed onto the surface of the semiconductor, an electrolyte contain redox mediator and counter electrode capable of regenerating the redox mediator. The efficiency of DSSC depends on each of the five components in terms of optimization and compatibility [1]. In 1991, Michael Grätzel and O'Regan at Swiss Federal Institute of Technology (EPFL), managed to build a DSSC device of efficiency 7.1% under air mass (AM) 1.5 irradiation. It was composed by nano crystalline titanium dioxide ($TiO_2$) thin film electrode having a microporous structure with large surface area, a Ru bipyridyl complex, and an iodine based redox electrolyte [2].

Among of the different oxide and non-oxide semiconductor photovoltaic, $TiO_2$ is one of the most efficient and economical photovoltaic that have been studied extensively in the application of DSSC due to its high photovoltaic activity, a long lifetime of photon-generated carrier, chemical inertness, low cost and non-toxicity. Generally, $TiO_2$ has three basic crystalline phases containing brookite, anatase and rutile. But, anatase titanium dioxide has attracted much attention because of its higher photovoltaic activity. Generally, sunlight includes almost 4% of ultraviolet light and 43% of visible light. Nevertheless, anatase titanium dioxide has a disadvantage of its intrinsic wide band gap ($E_g$ = 3.23 eV), which indicates that $TiO_2$ can be activated only under the ultraviolet radiation from sunlight with only a small portion of the solar energy, leading to its quite low solar energy usage [3].

The semiconductor needs UV light to excite the electrons from valence band to conduction band. Moreover, $TiO_2$ has disordered structures which is unfavorable for the transport of electrons. Thus, the photovoltaic conversion efficiency is limited [1]. Consequently, doping of $TiO_2$ is an alternative way to improve the efficiency of DSSC because it can easily shift the band edge and Fermi level of the materials. However, different elements show different result. Thus, to gain an optimize efficiency of DSSC, recent studies mostly classified on non-metals and metals element for doping with $TiO_2$. Therefore, this study focuses on metals element for doping.

In this paper, we have used CASTEP to evaluate the structural, electronic and optical properties of anatase $TiO_2$ and to determine the effect of Gd-doped anatase $TiO_2$ on the structural, electronic and optical properties.

## EXPERIMENTAL

*Computational Method*

The calculation of $TiO_2$ properties were carried out using the Cambridge Serial Total Energy Package (CASTEP) code [4], which is based on the density functional theory (DFT) [5, 6] which uses a total energy plane-wave pseudopotential method within the framework of Kohn–Sham DFT [7]. The exchange-correlation effects were treated within the local density approximation (LDA), generalized gradient approximation with the Perdew-Burke-Ernzerhof (GGA-PBE) and also with generalized gradient approximation with Perdew-Burke-Ernzerhof for solid (GGA-PBEsol) [8]. Special k-

points sampling integration over the Brillouin zone was employed by using the Monkhorst–Pack scheme [9]. The cut-off energy of 340 eV were applied and the k-point grid of 4x4x2 were set in Monkhorst-Pack scheme which is within the convergence value. The geometrical optimization set for anatase $TiO_2$ is 5.0 x $10^{-6}$ eV/atom for total energy, 0.01 eV/Å for maximum force, 0.02 GPa for maximum stress and 0.0005 Å for maximum displacement.

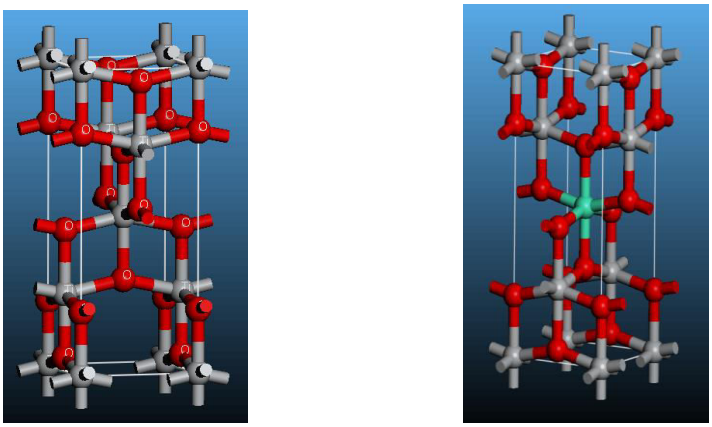

(a) (b)

Figure 1: Crystal structure of (a) pure anatase $TiO_2$ and Gd-doped anatase $TiO_2$

## RESULTS AND DISCUSSION

*Structural Parameter*

Crystalline $TiO_2$ has many polymorphs. One of it is anatase with space group, $I4_1/amd$. Figure 1 shows the crystal structure of (a) $TiO_2$ and (b) Gd-doped $TiO_2$ where the atom of O, Ti and Gd are indicated in these figure. The Ti atom that is located at the center is replaced with the Gd atom for the structure of Gd-doped $TiO_2$.

The structural parameter for optimized structures of the pure anatase $TiO_2$ and Gd-doped $TiO_2$ are obtained by using different functional and compared with the experimental one as shown in Table 1. The lattice parameter for pure anatase $TiO_2$ have been calculated using different functional which are LDA, GGA-PBE and GGA-PBEsol. The lattice constant ratio, *c/a* of pure anatase $TiO_2$ ranged from 2.5072 Å to 2.5669 Å and for Gd-doped $TiO_2$ is 2.5383 Å. The Gd-doped $TiO_2$ is optimized by only GGA-PBEsol. This is because, GGA-PBEsol have closest value of the lattice parameter with the experimental compared to other functional as also reported in the previous study [10,11]. The optimized cells parameter for pure anatase $TiO_2$ by using GGA-PBEsol are $a=b$=3.7735 Å $c$=9.6309 Å. But, for the Gd-doped $TiO_2$ the lattice parameter are $a=b$=3.8933Å $c$=9.8825Å which are larger than the parameter of the pure anatase $TiO_2$.

The valence atomic configuration are $3s^2$ $3p^6$ $3d^2$ $4s^2$ for Ti and $2s^2$ $2p^4$ for O. The valence atomic configuration of Gd is $4f^7$ $5d^1$ $6s^2$. The atomic position of the pure anatase $TiO_2$ and Gd-doped $TiO_2$ are shown in Table 2 and Table 3. The atomic position is stated for three axis *x, y* and *z*. For the pure anatase $TiO_2$, there are 4 atoms of Ti and 8 atoms of O. At the center of the $TiO_2$ is the Ti atom which at (0,0,0). For the Gd-doped $TiO_2$, there are 3 atoms of Ti, 8 atoms of O and 1 atom of Gd. The Gd is doped at the center which replace atom of Ti from the pure anatase $TiO_2$.

Table 1: Comparison of lattice parameter and volume for anatase $TiO_2$ and Gd-doped $TiO_2$

| Material | Functional | *a=b* (Å) | *c* (Å) | *c*/*a* | V (Å$^3$) |
|---|---|---|---|---|---|
| $TiO_2$ | LDA | 3.7409 | 9.5351 | 2.5489 | 133.4355 |
| | GGA-PBE | 3.8020 | 9.7592 | 2.5669 | 141.0739 |
| | GGA-PBEsol | 3.7735 | 9.6309 | 2.5522 | 137.1390 |
| Gd-doped $TiO_2$ | GGA-PBEsol | 3.8933 | 9.8825 | 2.5383 | 149.7820 |

Table 2: Atomic position of $TiO_2$ using GGA-PBEsol

| **Element** | **Atomic Position** | | |
|---|---|---|---|
| | x | y | z |
| Ti (1) | 0.0000 | 0.0000 | 0.0000 |
| Ti (2) | 0.5000 | 0.5000 | 0.5000 |
| Ti (3) | 0.0000 | 0.5000 | 0.2500 |
| Ti (4) | 0.5000 | 0.0000 | 0.7500 |
| O (1) | 0.0000 | 0.0000 | 0.2066 |
| O (2) | 0.5000 | 0.5000 | 0.7066 |
| O (3) | 0.0000 | 0.5000 | 0.4566 |
| O (4) | 0.5000 | 0.0000 | 0.9566 |
| O (5) | 0.5000 | 0.0000 | 0.5434 |
| O (6) | 0.0000 | 0.5000 | 0.0434 |
| O (7) | 0.5000 | 0.5000 | 0.2934 |
| O (8) | 0.0000 | 0.0000 | -0.2066 |

Table 3: Atomic position of Gd-doped $TiO_2$ using GGA-PBEsol

| Element | Atomic Position | | |
|---|---|---|---|
| | x | y | Z |
| Ti (1) | 0.000081 | 0.000159 | 0.000008 |
| Ti (2) | -0.001033 | 0.500462 | 0.231879 |
| Ti (3) | 0.500609 | -0.000310 | 0.768109 |
| Gd (1) | 0.499037 | 0.499218 | 0.500008 |
| O (1) | 0.000139 | 0.000340 | 0.197434 |
| O (2) | 0.500403 | 0.499836 | 0.732569 |
| O (3) | -0.000759 | 0.500300 | 0.430656 |
| O (4) | 0.500253 | 0.000007 | 0.965077 |
| O (5) | 0.500942 | -0.000597 | 0.569355 |
| O (6) | -0.000118 | 0.500151 | 0.034934 |
| O (7) | 0.500022 | 0.500367 | 0.267438 |
| O (8) | 0.000425 | 0.000068 | 0.802553 |

Table 4 shows the average bonding length of the atoms in the pure anatase $TiO_2$ and Gd-doped TiO. The average bonding length for pure anatase $TiO_2$ in all the functionals are not much different between each other. The O-O bonding length of pure anatase $TiO_2$ ranged from 2.60343 Å to 2.64652 Å and for O-Ti from 1.94399 Å to 1.97862 Å. The average bonding length of atoms in Gd-doped $TiO_2$ is larger than the pure $TiO_2$ (GGA-PBEsol). The average bonding length of Gd-doped $TiO_2$ for O-O is 2.65924 Å, for O-Ti is 1.964.81Å and for O-Gd is 2.18121 Å. The average bonding length increases due to the atomic radius of the Gd which larger than the Ti atom.

Table 4: Average bonding length of O-O and Ti-O for anatase $TiO_2$ and O-Gd for Gd-doped $TiO_2$

| Material | Functional | Average Bonding Length (Å) | | |
|---|---|---|---|---|
| | | O-O | O-Ti | O-Gd |
| $TiO_2$ | LDA | 2.60343 | 1.94399 | - |
| | GGA-PBE | 2.64652 | 1.97862 | - |
| | GGA-PBEsol | 2.62582 | 1.96101 | - |
| Gd-doped $TiO_2$ | GGA-PBEsol | 2.65924 | 1.96481 | 2.18121 |

*Electronic Properties.*
One important factor to study about DSSC and the properties of the $TiO_2$ as one of the main component in DSSC is the band structure. Figure 1 shows the band structure of $TiO_2$ and Gd-doped $TiO_2$ with different functional. The calculated band gap for $TiO_2$ is

2.125 eV, 2.143 eV and 2.153 eV by using LDA, GGA-PBE and GGA-PBEsol respectively. Compared to the experimental band gap, the band gap of $TiO_2$ is 3.2 eV [12]. Eventhough the range between the experimental and the theoretical is large but the calculated band gaps agree with previous theoretical report. The small band gap of theoretical due to the under-estimation which is explained by the DFT limitation, namely the discontinuity in the exchange-correlation potential is not taking account and it will not affect the results' relative accuracy [13].

Figure 2(a) shows that the calculated minimal band gap of the pure anatase $TiO_2$ by LDA is 2.125 eV which it is indirect; the minimum conduction bands is at G and the top of the valence bands is near M. Figure 2(b) and (c) show the same indirect gap but with different band gap value. The band gap of Gd-doped $TiO_2$ became smaller to 0.247 eV compared to pure $TiO_2$ as shown in Figure 2(d).

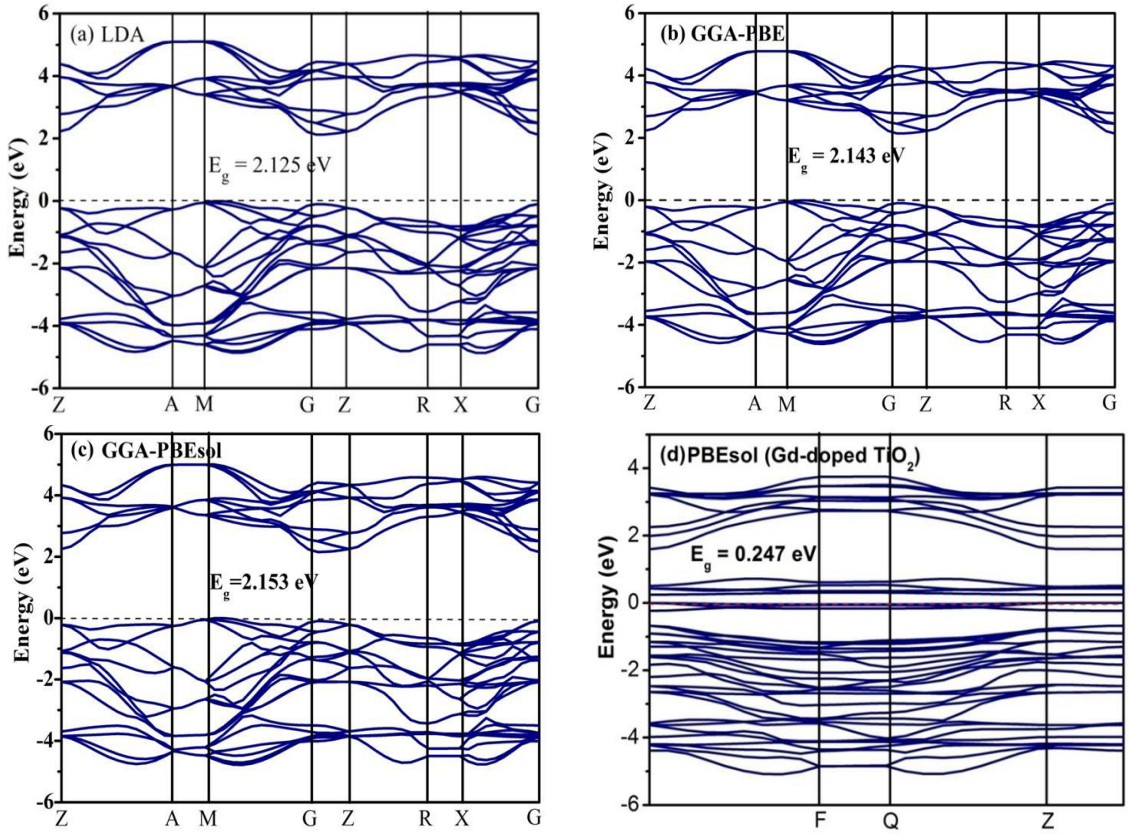


Figure 2: Calculated band structures of $TiO_2$ using (a) LDA (b) GGA-PBE and (c) GGA-PBEsol and (d) Gd-doped $TiO_2$ using PBEsol

In Table 5, the band gap of $TiO_2$ became narrower when doped with Gd which from 2.153 eV to 0.247 eV by comparing with the same functional of GGA-PBEsol. The calculated band gap of the Gd-doped $TiO_2$ is 0.65 eV by using GGA-PBE [3]. Thus, it shows that after $TiO_2$ been doped, the band gap will became narrower. Based on

equation $E=hc/\lambda$, energy gap is inversely proportional to the wavelength [2]. As the energy gap is small, longer wavelength can be absorb and easier for the electron to excited from the valence band to the conduction band.

Table 5: The comparisons of band gap of $TiO_2$ and Gd-doped $TiO_2$ between functionals and experiment

| Materials | Method | Band gap (eV) |
|---|---|---|
| Anatase $TiO_2$ | LDA | 2.125 |
| | GGA-PBE | 2.143 |
| | GGA-PBEsol | 2.153 |
| | Experiment | 3.2 |
| Gd-doped $TiO_2$ | GGA-PBEsol | 0.247 |
| | Experiment | 3.11 |

After optimized the structure, the total and partial density of states (DOS) of pure anatase $TiO_2$ and Gd-doped $TiO_2$ also been calculated to understand the chemical bonding of those materials. The energy interval for the calculated total DOS is within ($E_F$ -6 eV) to ($E_F$ +6 eV) as shown in Figure 3. The dashed line in the DOS indicates the Fermi level. For pure anatase $TiO_2$, the valence band and conduction band are composed of O 2*p* states and Ti 3*d* states. Thus, the +2 eV to the right is the conduction band and from the 0 eV to the left is the valence band. Primarily, the conduction bands formed by Ti atoms and the valence bands are given by the O and Ti atoms [14].

Figure 3(d) shows the partial density of states (PDOS) of Gd-doped $TiO_2$. Compared to the pure anatase $TiO_2$, the 4*f* states of Gd can be seen which indicated with green colour line. After doping, the valence band around the Fermi level is wider than the pure anatase $TiO_2$ and the conduction band top has shifted up. These will explain the narrowing of band gap of Gd-doped $TiO_2$. The new valence state level from Gd 4*f* states are formed and mainly distributed in the middle of the forbidden band. Thus, it make the gap became narrower.

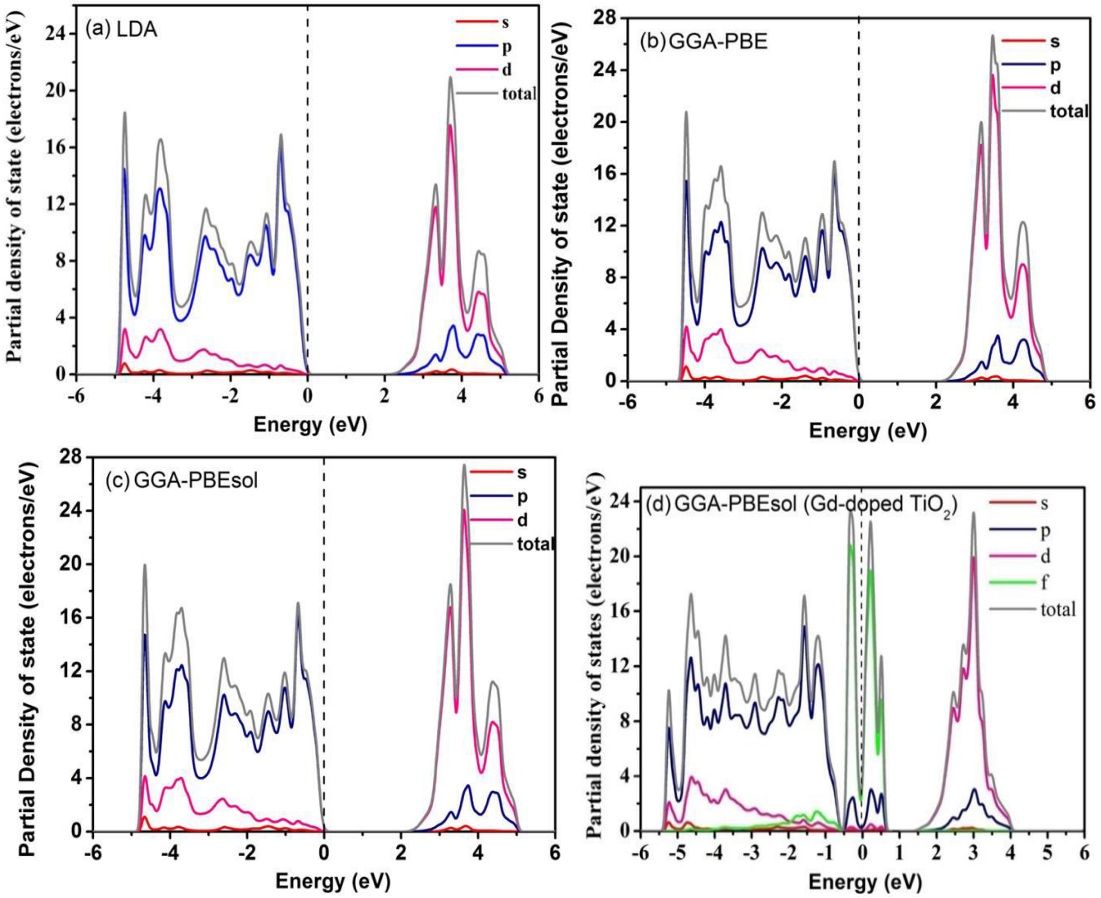


Figure 3: Partial density of states $TiO_2$ using (a) LDA (b) GGA-PBE (c) GGA-PBEsol and (d) Gd-doped $TiO_2$ using GGA-PBEsol

*Optical Properties*

Pure anatase $TiO_2$ can absorb light that have wavelength in UV region. This can be seen in Figure 4 which show the graph of absorption against energy for anatase $TiO_2$ that had been calculated using all three functionals and in Figure 5 (a) which shows the graph of absorption against wavelength. Compared to all functional, the graphs of absorption spectrum are almost similar. The ranges of wavelength for UV region are from 100 nm to 400 nm. The optical properties are related to the electronic properties, small band gap gives more sunlight can be absorbed.

Figure 5 (a), shows that the comparison of optical absorption spectrum of pure anatase $TiO_2$ and Gd-doped $TiO_2$ using GGA-PBEsol. The absorption spectrum of Gd-doped $TiO_2$ shifted to the right compared to the pure anatase $TiO_2$ which shows that light can be absorb at the range of visible light and also in infrared which the wavelength of visible light are between 390 nm to 700 nm . As wider range of spectrum after doping, it explained how the doping effect improves the DSSC. Electron can be excited eventhough the energy of photon absorbed is very low.

Figure 5 (b) shows that the Gd-doped $TiO_2$ shifted the optical absorption to lower energy. Related to the bottom conduction band can serve as effective traps of the excitation energy. Thus, it is possible to excite $Gd^{3+}$ luminescence in anatase $TiO_2$ band-to-band excitation of the host itself. Based on Figure 2, shows that the conduction band energy level locating between the LUMO level of dye which help the transition of electrons from dye molecule to the electrode of DSSC.

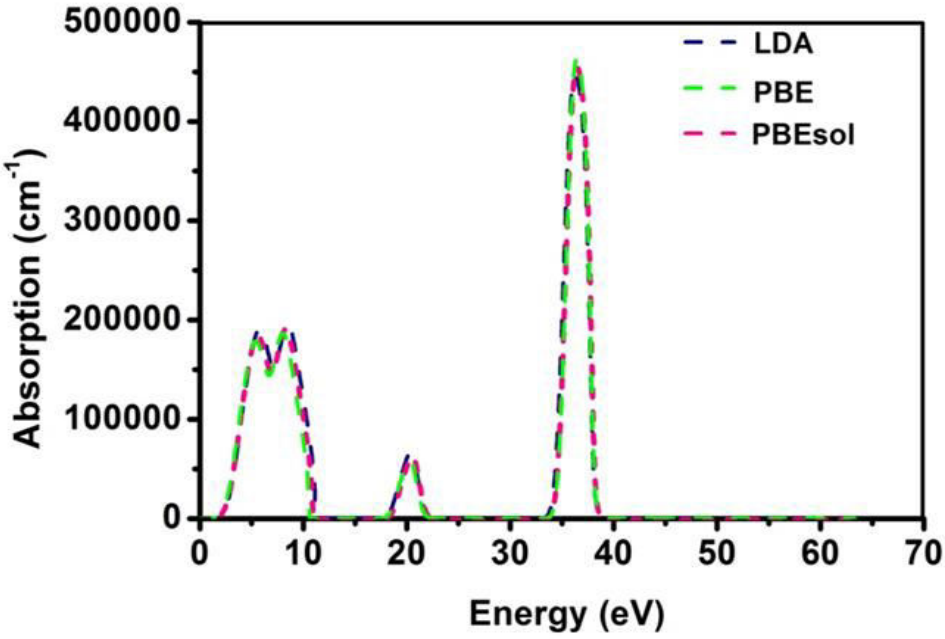


Figure 4: Absorption spectrum and energy of pure anatase $TiO_2$

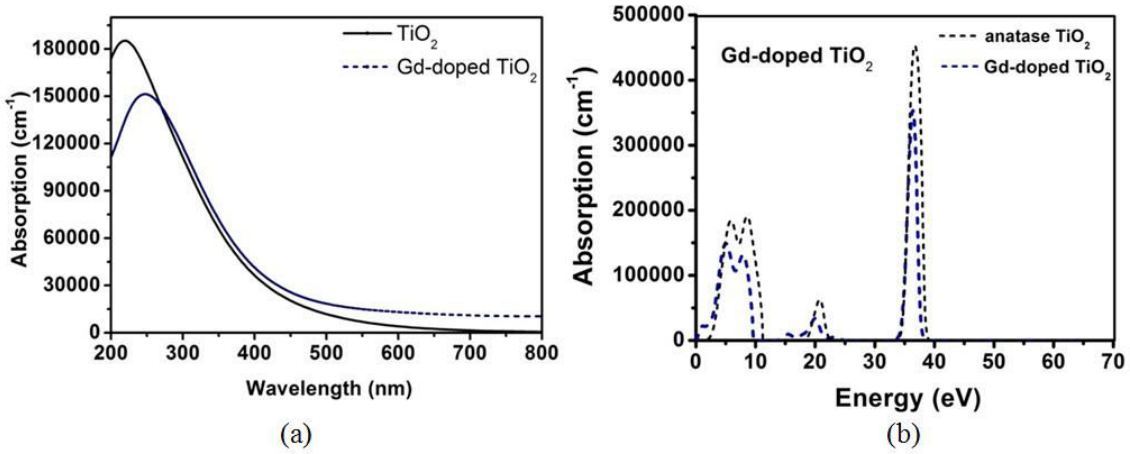


Figure 5 (a) Absorption spectrum and wavelength of pure anatase $TiO_2$ and Gd-doped TiO2 (b) Absorption spectrum and energy of pure anatase TiO2 and Gd-doped TiO2 using GGA-PBEsol

## CONCLUSION

In conclusion, the structural, electronic properties and optical properties of pure anatase $TiO_2$ were calculated through the first-principle study using LDA, GGA-PBE and GGA-PBEsol from CASTEP software. The lattice parameters of pure anatase $TiO_2$ calculated by using GGA-PBEsol were in better agreement with the experimental value. The appearance of the Gd-4*f* states within the band gap explained the narrowing of the band gap of Gd-doped $TiO_2$. It can also influent the energy band structure and forming hybrid orbital, which then effectively improve the photocatalytic activity of $TiO_2$. The optical absorption shifted from UV region to visible light region so that more energy from the sunlight can be absorbed where the minimal energy to excite electron is small due to the longer wavelength. The properties from first principle study shown in Gd-doped $TiO_2$ can explain the improvement of the efficiency in the DSSC because the increasing of light harvesting from the doping effect in $TiO_2$.

## ACKNOWLEDGEMENT

The authors would like to thank to Universiti Teknologi MARA (UiTM) and Ministry of Education Malaysia (MOE) for FRGS and RAGS for funding this research.

## REFERENCES

[1]. Z. Yi, L. Hong, S.DeHui, L. CaiXia, D. MingMing, L. Wen. *Journal of Materials Engineering and Performance,* **20** 2011-1319 (2010)
[2]. M. Mikami, S. Nakamura, O. Kitao, H. Arakawa and X. Gonze, *Jpn. J. Appl. Phys*. **39** 847-850 (2000)
[3]. X. Ruiqing, Y. Lanfang, L. Lin, W. Shuo, T. Linlin, F. Xueling, *Advanced Materials Research,* **156-157** 1385-1388 (2011)
[4]. S. J. Clark, M. D. Segall, C. J. Pickard, P. J. Hasnip, M. I. J. Probert, K. Refson, M. C. Payne, *Zeitschrift für Kristallographie.* **220** 567 (2005)
[5]. P. Hohenberg and W. Kohn, *Phys. Rev.* **136** B864 (1964)
[6]. W. Kohn and L.J. Sham, *Phys. Rev.* **140** A1133 (1965)
[7]. M.K. Yaakob, N.H. Hussin, M.F.M. Taib, T.I.T. Kudin, O.H.Hassan, A.M.M. Ali, M.Z.A. Yahya, *Integr. Ferroelectr.* **155** 15–22 (2014)
[8]. M.D. Segall, P.J.D Lindan, M J Probert, C.J. Pickard, P.J. Hasnip, S.J. Clark, M.C. Payne, *J. Phys.: Condens. Matter* **14** 2717–2744 (2002)
[9]. H.J. Monkhorst, J.D. Pack, *Phys. Rev. B* **13** 5188 (1976)
[10]. M.F.M. Taib, M.K. Yaakob, F.W. Badrudin, T.I.T. Kudin, O.H. Hassan, M.Z.A. Yahya, *Ferroelectrics.* **459** 134–142 (2014)
[11]. M.K. Yaakob, M.F.M. Taib, M.S.M. Deni, M.Z.A. Yahya, *Integrated Ferroelectrics: An International Journal,* **155** (1) 134-142 (2014)
[12]. Q. Liua, Y. Zhoua, Y. Duan, M. Wang, Y. Lin, *Electrochimica Acta* **95** 48– 53 (2013)
[13]. Z. Xi, L. Fang, H. Qiu-Liu, Z. Gang, W. Zhong-Sheng. *J. Phys. Chem.* **115** 12665-12671 (2011)

[14]. S.J. Clark, M.D. Segall, C.J. Pickard, P.J. Hasnip, M.J. Probert, K. Refson, M.C. Payne, *Journal of Alloys and Compounds*. **611** 125–129 (2014)